

## Influence of thermal annealing and deposition conditions on structure and physical-mechanical properties of multilayered nanosized TiN/ZrN coatings

**Abstract.** Nanostructured multilayered TiN/ZrN coatings were fabricated using vacuum-arc deposition method. Amount of layers was 134-533; average bilayer thickness was 20-125 nm depending on deposition conditions. Good planarity of nanoscale bilayers were observed. Regularities of phase-structure changes in surface layers under the influence of aggressive oxygen atmosphere and high temperature (700 °C) annealing were established as a model of critical working conditions. Bilayer thickness influence on hardness was explored. Maximum hardness was 42 GPa.

**Streszczenie.** Nanostrukturalne wielowarstwowe powłoki TiN/ZrN otrzymano używając metody próżniowo-lukowego osadzania. Ilość warstw wynosiła 134-533; średnia grubość dwuwarstwowa wynosiła 20-125 nm zależnie od warunków osadzania. Zaobserwowano dobrą planarność podwójnych warstw w nanoskali. Określono prawidłowości zmian struktury fazowej w warstwach powierzchniowych pod wpływem agresywnej atmosfery utleniającej oraz wysokiej temperatury (700 °C) wygrzewania jako model krytycznych warunków pracy. Zbadano wpływ grubości podwójnych warstw na twardość. Maksymalna twardość wynosiła 42 GPa. (Wpływ wygrzewania oraz warunków osadzania na strukturę oraz fizyko-mechaniczne właściwości nanowymiarowych wielowarstwowych powłok TiN/ZrN)

**Keywords:** vacuum-arc deposition, multilayered TiN/ZrN coatings, structure of surface layers, mechanical properties.

**Słowa kluczowe:** lukowo-próżniowe osadzanie, powłoki wielowarstwowe TiN/ZrN, struktura powierzchni warstw, właściwości mechaniczne.

### Introduction

Fabrication of multilayered systems based on nitrides of refractory metals is one of the perspective ways of improving of physical-mechanical properties of the coatings. Combination of layers from different nitrides allows receiving unique properties of the coatings, such as superhardness, wear and oxidation resistance, significantly better than properties of the appropriate single-layered coatings. Such coatings could be used as cutting tools and friction pairs of machinery with improved lifetime [1].

It was showed in the works [2-7], that 20-30 nm layers, consisted of nitrides of refractory metals, are perspective for improving of the mechanical properties of multilayered coatings. Coatings, made of two periodically repeated layers of nitrides of refractory metals have much higher hardness in comparison with appropriate single-layered coatings, due to stresses that prevent movement of dislocations [7].

Thus, combination of TiN and ZrN layers with high hardness in one multilayered coating allow significant increasing of its hardness due to forming of a large amount of strongly coupled interphase boundaries.

### Experimental details

The multilayered coatings were deposited using vacuum-arc evaporation method from two evaporators, one of which contained titanium of the grade VT1-00 (Fe < 0.12%, C < 0.05%, Si < 0.08%, N < 0.04%, O < 0.1, H < 0.008, Ti was in the range 99.5 – 99.9), the second – zirconium, which was fabricated using the method of electron beam melting using BULAT-6 deposition device, which allows deposition of nanostructured coatings in pulsed mode with variable pulse amplitude and pulse frequency [7, 8]. The coatings were deposited on the A 570 Grade 36 steel ( $R_a = 0.09 \mu\text{m}$ ) polished substrates under different deposition regimes. Size of the substrates was 15x15x2.5 mm. The arc current during deposition was 100 A, the nitrogen pressure in the deposition chamber was  $3 \cdot 10^{-3}$  Torr, the distances from evaporators to substrate

were 250 mm, the substrate temperature was 250-350°C, deposition speed of ZrN and TiN layers was around 3 nm/sec and 2 nm/sec respectively. Negative bias potential -150 V was applied to the substrates. Such relatively low substrate temperature allowed us to fabricate homogeneous coatings with good enough planarity.

We prepared three series of samples with different bilayer thickness and total thickness of the coatings.

First series of samples had a TiN/ZrN bilayer thickness  $\lambda \approx 40$  nm, total thickness  $h$  was 13  $\mu\text{m}$ . Second and third series had the next parameters:  $\lambda \approx 70$  nm,  $h \approx 14 \mu\text{m}$  and  $\lambda \approx 250$  nm,  $h \approx 14 \mu\text{m}$  respectively. Amount of layers was 533 for first, 233 for second and 134 for third series of samples.

Annealing of the samples were done in the vacuum chamber, pressure in it was  $10^{-5}$  Torr, in the oxygen atmosphere with the pressure  $5 \cdot 10^{-3}$  Torr [9-12].

Surface morphology, diffraction patterns of fracture and wear tracks were investigated using scanning electron microscope FEI Nova NanoSEM 450. Phase-structure state was explored using diffractometer DRON-3M in Cu-K $\alpha$  irradiation.

Tribological tests were done using the scheme "ball-disc". "Tribometer", CSM Instruments was used as a friction device. Ball with a 6.0 mm diameter was used as a counterbody, it was fabricated from sintered certified material – Al<sub>2</sub>O<sub>3</sub>. Load was 6.0 N, sliding speed was 10 cm/sec. Tests fitted the international standards ASTM G99-959, DIN50324 and ISO 20808.

Hardness of the coatings were measured using DM-8 hardness-meter by micro-Vickers methodology. Load on the indenter was 0.2 N.

### Results and discussion

Typical fragment of the diffraction pattern of the multilayered sample is presented on the Fig. 1. Thickness of the informative layer was around 4  $\mu\text{m}$ . We clearly see layers with cubic TiN and ZrN phases (of the NaCl structure type) without preferred orientation of crystallites in the

surface layers. Increasing of the period  $\lambda$  led to increasing of the TiN layers specific contribution – it is seen from changes in the intensity of the peaks of TiN and ZrN phases (see Fig. 1a and 1b). Increasing of the deposition time and, as a result, bilayer thickness as well as total period of the multilayered system led to changes of the lattice period of nitride phases in the layers. Lattice period decreased with increasing of the TiN-layers thickness from 0.4241502 nm (deposition time was 20 sec,  $\lambda \approx 70$  nm) to 0.4238870 nm (deposition time was 40 sec,  $\lambda \approx 250$  nm). Changes for ZrN layers were not so big: from 0.4581055 nm (deposition time was 20 sec) to 0.4581046 nm (deposition time was 40 sec).

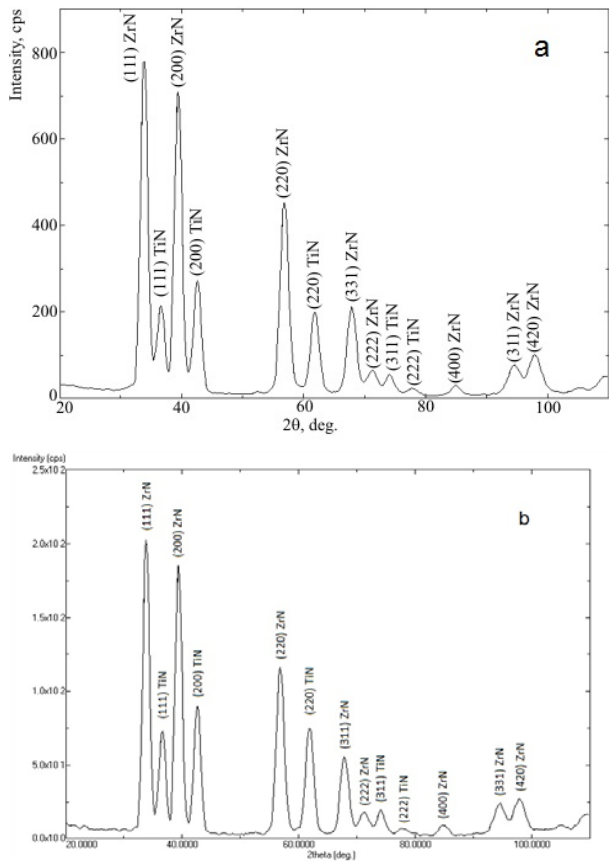


Fig.1. Diffraction patterns of the coatings from the second series with  $\lambda \approx 70$  nm (a) and third series,  $\lambda \approx 250$  nm (b).

Annealing in the oxygen atmosphere led to oxidation of the surface layers [13, 14] and to forming of dioxides as the main phases: –  $\text{TiO}_2$  (with tetragonal rutile-type crystal system; basic, up to 95 vol.% in the layers based on titanium) and anatase (5 vol.% and less). We can determine anatase (DB card number 5000223) on the diffraction spectra (Fig. 2a) using the most strong first line on the angle  $2\theta \approx 25.36$  degrees. Diffraction spectrum is shown for the rutile (DB card number 9007531) see Fig. 2a. Only one type of dioxide  $\text{ZrO}_2$  (arkel having a cubic crystal system, DB card number 5000038) was formed in the zirconium nitride layers after oxidation.

Layered X-Ray analysis showed that after removal of the surface layer (thickness of about 5 microns) by polishing, we could see dioxides only in the subsurface layer of the coating. In more thick layers (Fig. 2b) we did not find oxides whereas nitrides are characterized by preferred orientation of crystallites with the [111] axis, perpendicular to the plane of growth. Therefore, preferred orientation with the [111] axis was formed at the beginning stage of growth for both TiN and ZrN crystallites. Increasing of the total thickness of the coatings and relaxation of the compressive

stresses led to disorientation of crystallites, i.e. preferred orientation was not observed.

Using XRD analysis data (Fig. 2) we could assume, that due to disorientation of crystallites in the surface layers and low compressive stresses, oxygen from the atmosphere penetrates into the subsurface layers during deposition. It formed stable dioxide phases of metals due to easier diffusion by intercrystallite ways. In more deep layers, corresponding to the beginning stages of growth, [111] texture of growth appeared due to compressive stresses [15 – 17]. This texture prevents diffusion of oxygen into such layers due to high packing density of the plane (111), so there are not enough oxygen to form dioxide phases.

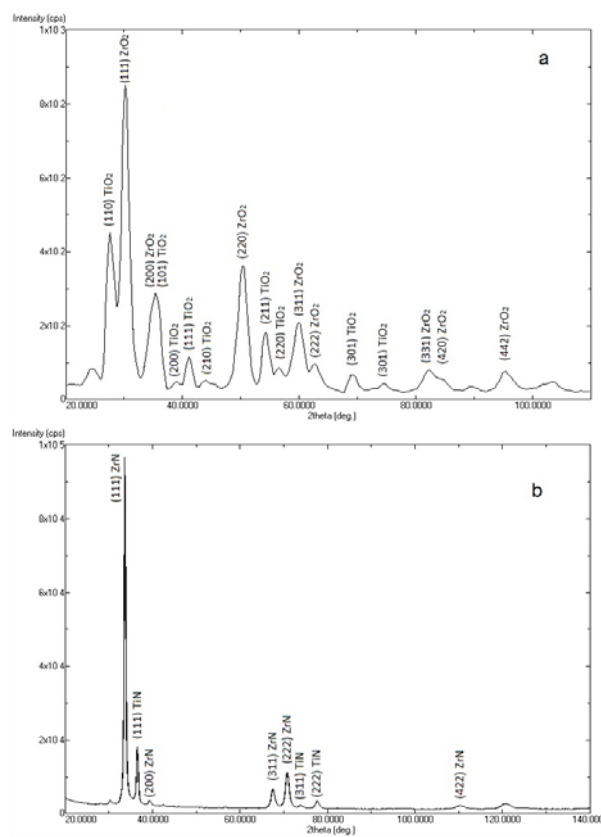


Fig.2. Diffraction patterns of the TiN/ZrN coatings ( $\lambda \approx 70$  nm), after thermal annealing under the temperature of 700°C for one hour: a – from the surface without polishing, b – after polishing of the oxidized surface on the depth of 5  $\mu\text{m}$ .

Transmission electron microscopy (TEM) allowed providing detailed analysis of changes in the surface layers after oxidation. Electron images of the cross-sections of the TiN/ZrN samples from different series are presented on the Fig. 3. Good planarity was observed even for the thinnest layers of the coatings from the first series (Fig. 3a and 3b). High continuity of the coatings and the lack of inhomogeneity, such as droplet fractions, are also typical for investigated samples.

Energy-dispersion spectra is presented on the Fig. 4a, and it is typical for all series of samples. Stoichiometry of the composition of the TiN/ZrN coatings can be seen from it.

Changes of elemental composition in the surface layers were observed after annealing. Amount of oxygen atoms in working atmosphere was 35 at.%, see Fig. 4b. Penetration of oxygen atoms into nitride layers, as well as titanium and zirconium dioxides forming in the surface layers significantly changed the structure of surface layers due to increasing of

its volume after substitution of nitrogen atoms by oxygen atoms and forming of dioxide phases.

Comparison of electron microscopy images of the structural state of the layers in the multilayered TiN/ZrN coatings with total amount of layers 134 (Fig. 5) showed, that increasing of the volume fraction led to bending of layers, stratification with separation and loss of strength during oxidation (Fig. 5c and 5d). We observed dome-like discontinuities in the areas of partial separation of layers (Fig. 5d) on the surface. Comparison of structures 1 and 2 on the Fig. 5 showed that main volume changes took place in the titanium-based layers, whose thickness increased from 80 nm to 110 nm, i.e. by 37.5%. Thickness of zirconium-based layers increased from an average value 120 nm before annealing to 135 nm after annealing during oxidation (Fig. 5a and 5c), i.e. by 12.5%. Wherein, columnar character of the grain structure is clearly seen in zirconium-based layers, that is why they become quite fragile. High density was observed in titanium-based layers, so we can assume, that this layers are subjected to compression and compaction as a result of oxidation, despite the relatively high increasing of the thickness. Thus, compensating tensile strain in the layers of the plane of growth should be created in titanium-based layers, which determines their tendency to brittle fracture. Interphase boundary is the main area of separation; it can be explained by decreasing of the adhesive bonds during forming of phases with different crystal lattices (cubic in zirconium-based layers and tetragonal in titanium-based layers) due to oxidation.

Thus, unlike single-layer coating or coating with few layers, only subsurface layers are susceptible to phase changes (in multilayered coating with amount of nanoscale layers more than 100) even in the case of severe operation conditions in active oxygen atmosphere, thereby preventing main structural state of inner carrier layers from changes.

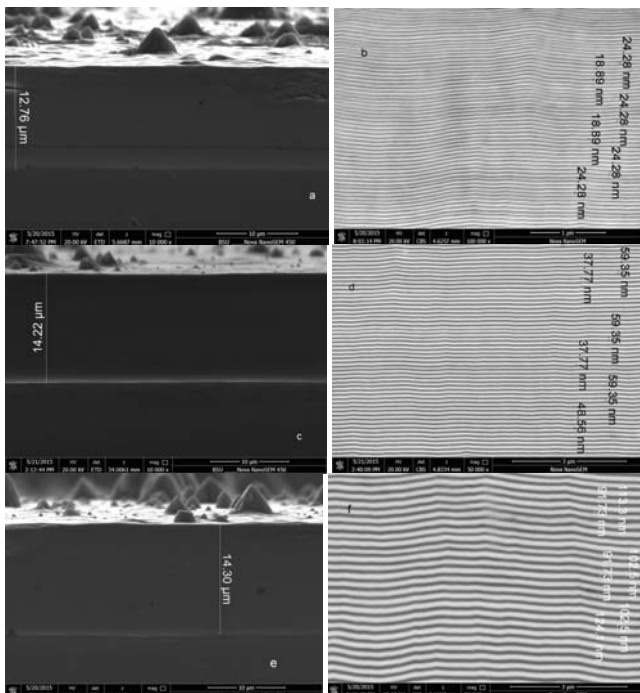


Fig.3. Electron images of the cross-sections of the TiN/ZrN samples (general view of the cross-section and magnified fragment) with amount of layers 533 (a and b), 233 (c and d) and 134 (e and f)

Hardness is well known as a universal characteristic, which allow rapidly estimating of mechanical properties of the coatings [16, 17]. We defined hardness using microindentation method, and hardness was around  $H \approx 42$

GPa for the first series of samples,  $H \approx 38$  GPa and  $H \approx 36$  GPa for the second and the third series of samples accordingly. Thus, high hardness is typical for all series of samples with different bilayer thickness, so such coatings are perspective for using as protective ones. In this connection, it was also necessary to provide tribological tests to determine basic mechanical properties upon contact of the coating with counterbody.

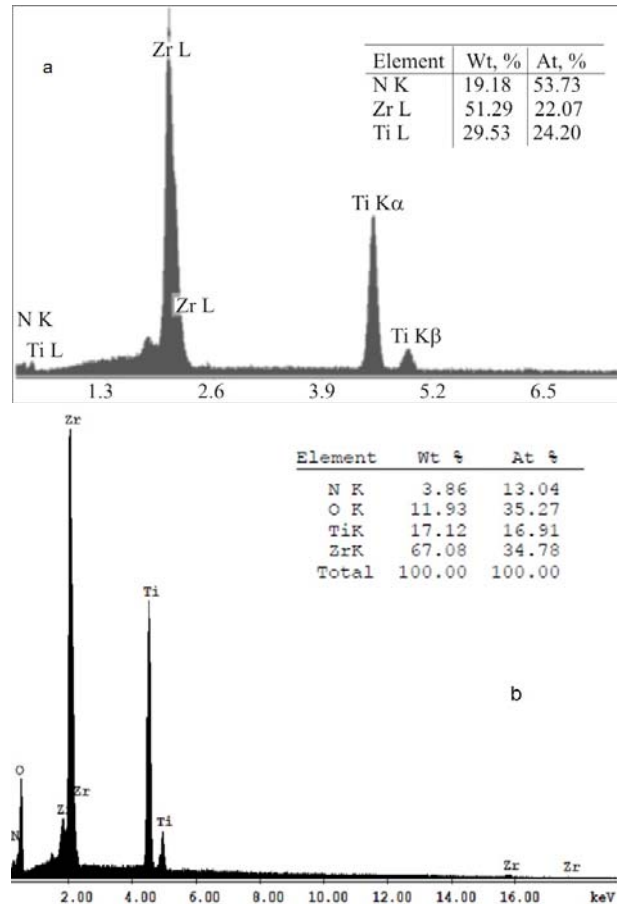


Fig.4. Energy-dispersion patterns with elemental composition of the TiN/ZrN coatings before (a) and after (b) annealing in the oxygen atmosphere under the temperature of 700°C.

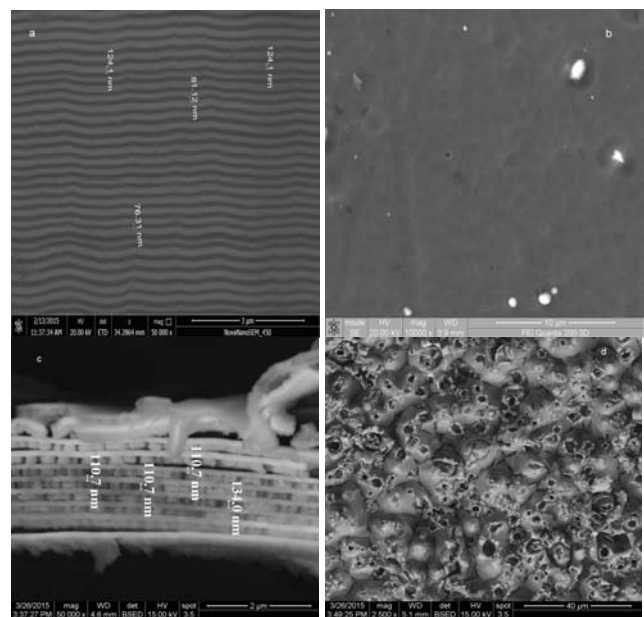


Fig.5. Image of the cross-section and surface of the coating from the third series before (a, b) and after (c, d) annealing.

Results of tribological tests of multilayered samples with different bilayer thickness under room temperature are presented in Table 1.

Table 1. Tribological properties of the multilayered TiN/ZrN coatings

Series No.	Friction Coefficient		Wear factor, $\text{mm}^3 \times \text{N}^{-1} \times \text{mm}^{-1}$	
	Starting moment	During tests	Counterbody ( $\times 10^{-6}$ )	Samples ( $\times 10^{-5}$ )
1	0.59	1.0	1.9	1.3
2	0.62	1.2	2.0	1.5
3	0.62	1.1	2.2	1.4

It is clearly seen from the table, that fabricated multilayered coatings have high wear coefficient paired with  $\text{Al}_2\text{O}_3$  counterbody.

Fig. 6 shows the images of friction tracks for TiN/ZrN samples with different bilayer thickness.

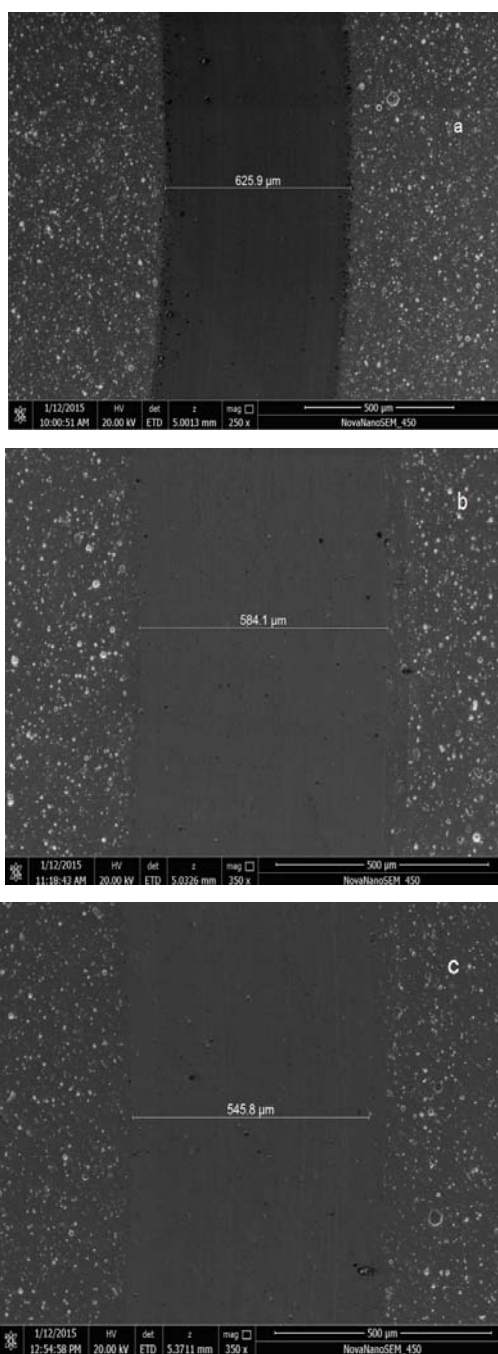


Fig.6. Friction tracks of the multilayered TiN/ZrN coatings: sample from the first (a), second (b) and third (c) series.

One could see that friction tracks are characterized by absence of burrs, cleavages and radial cracks, indicating the high quality and adhesive strength of coatings.

All fabricated coatings have good wear resistance, average values of the reduced wear were  $(1.3 - 1.5) \times 10^{-5} \text{ mm}^3 \times \text{N}^{-1} \times \text{mm}^{-1}$ . Wear of the counterbody was rather small  $(1.9 - 2.2) \times 10^{-6} \text{ mm}^3 \times \text{N}^{-1} \times \text{mm}^{-1}$ . Chipping, cracking and peeling of coatings were not observed during friction tests. We found good adhesion of the coatings to substrates. There were no plastic deformation during tests; the observed wear is rather typical for soft metals [10, 11].

Fig. 7 shows values of friction coefficients for multilayered TiN/ZrN coatings.

Samples from the second series had the highest values of the friction coefficient  $\mu$  (curve 2 on Fig. 7). There was a great difference between values of friction coefficient for the first and third series on the distance from 0 to 300 meters. Friction coefficient  $\mu$  for the samples from the third series sharply increased to the value 1.2 and stayed on this level along the length of testing area. Values of  $\mu$  for the samples from the first series monotonically increased along the friction distance and are equal to the values for the third series. Friction coefficient of the samples from the second series sharply achieved the value 1.2 and then slowly monotonically increased to the value 1.3.

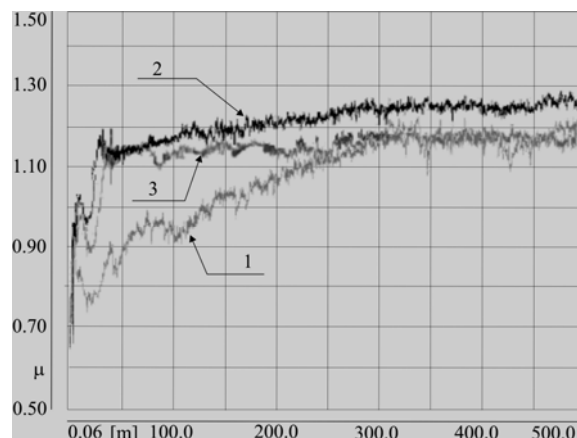


Fig.7. Friction coefficients of the TiN/ZrN coatings: samples from the first (1), second (2) and third (3) series.

Friction coefficient  $\mu$  significantly depended on bilayer thickness and total thickness of the coatings. The lowest friction coefficient was observed for the samples from the first series with 20 nm bilayer thickness and  $\lambda \approx 40 \text{ nm}$ . The highest values of friction coefficient were observed for the samples of the second series with  $\lambda \approx 70 \text{ nm}$ .

### Conclusions

1. Vacuum-arc deposition method was used for fabrication of nanoscale two-phase multilayered TiN/ZrN coatings with good planarity of layers.
2. Increasing of the thickness of TiN/ZrN bilayer (bias was -150 V) led to changes from preferred orientation of the crystallites with the axis [111] to nontexturized state.
3. Texture [111] in the surface layers prevented the coatings from oxidation during high-temperature annealing under the temperature  $700^\circ\text{C}$  in oxygen atmosphere.
4. All fabricated coatings demonstrated high hardness 38 – 42 GPa.
5. The highest hardness 42 GPa, as well as the lowest abrasive wear  $1.3 \times 10^{-5} \text{ mm}^3 \times \text{N}^{-1} \times \text{mm}^{-1}$  and counterbody wear  $1.9 \times 10^{-6} \text{ mm}^3 \times \text{N}^{-1} \times \text{mm}^{-1}$  were observed in the TiN/ZrN coatings with the smallest

bilayer thickness 20 nm due to significant influence of the sizes of the interphase boundary.

*This work was done under the aegis of Ukrainian complex state budget programs "Development of material science foundations of structure engineering of vacuum-plasma superhard coatings with required functional properties" (registration number 0115U000682) and "Physical principles of plasma technologies for complex treatment of multicomponent materials and coatings" (registration number 0113U000137c).*

#### REFERENCES

- [1] Pogrebnjak A.D., Beresnev V.M. Nanocoatings Nanosystems Nanotechnologies, *Bentham Sci. Publ.*, (2012), 147 p.
- [2] Abadias G., Michel A., Tromas C., Jaouen C., Dub S.N., Stress, interfacial effects and mechanical properties of nanoscale multilayered coatings, *Surf. Coat. Technol.*, 202 (2007), 844-853.
- [3] Vladescu A., Kiss A., Popescu A., Braic M., Balaceanu M., Braic V. et al., Influence of bilayer period on the characteristics of nanometre-scale ZrN/TiAlN multilayers, *J. Nanosci. Nanotechnol.*, 8 (2008), 717-738.
- [4] Stueber M., Holleck H., Leiste H., Seemann K., Ulrich S., Ziebert C., Concepts for the design of advanced nanoscale PVD multilayer protective thin films, *J. Alloy Compd.*, 483 (2009), 321-354.
- [5] Poliak N.I., Anishchik V.M., Valko N.G., Karwat C., Kozak C., Opielak M., Mechanical properties of Zn-Ni-SiO<sub>2</sub> coating deposited under X-ray irradiation, *Acta Phys. Pol. A*, 125 (2014), No 6, 1415-1417.
- [6] Chen S.-F., Kuo Y.-C., Wang C.-J., Huang S.-H., Lee J.-W., Chan Y.-C., Chen H.-W., Duh J.-G., Hsieh T.-E. The effect of Cr/Zr chemical composition ratios on the mechanical properties of CrN/ZrN multilayered coatings deposited by cathodic arc deposition system, *Surf. Coat. Technol.*, 231 (2013), 247-252
- [7] Pogrebnjak A.D., Eyidi D., Abadias G., Bondar O.V., Beresnev V.M., Sobol O.V., Structure and properties of arc evaporated TiN/MoN multilayered systems, *Int. J. Refract. Met. Hard Mater.*, 48 (2015), 222-228.
- [8] Pogrebnjak A.D., Yakushchenko I.V., Bagdasaryan A.A., Bondar O.V., Krause-Rehberg R., Abadias G., Chartier P., Oyoshi K., Takeda Y., Beresnev V.M., Sobol O.V., Microstructure, physical and chemical properties of nanostructured (Ti-Hf-Zr-V-Nb)N coatings under different deposition conditions, *Mater. Chem. Phys.* 147 (2014), No 3, 1079-1091.
- [9] Ivashchenko V, Veprek S., Pogrebnjak A., Postolnyi B. First-principles quantum molecular dynamics study of Ti<sub>x</sub>Zr<sub>1-x</sub>N(111)/SiN<sub>y</sub> heterostructures and comparison with experimental results. *Sci. Technol. Adv. Mater.*, 15 (2014), No 2, Article number 025007.
- [10] Pogrebnjak A.D., Shpak A.P., Azarenkov N.A., Beresnev V.M. Structures and properties of hard and superhard nanocomposite coatings, *Phys. Usp.*, 52 (2009), nr 1, 29 – 54.
- [11] Pogrebnjak A. D. Structure and Properties of Nanostructured (Ti-Hf-Zr-V-Nb)N Coatings, *J. of Nanomater.* (2013), ID 780125, 12 pages.
- [12] Koltunowicz T.N., Zhukowski P., Bondariev V., Saad A., Fedotova J.A., Fedotov A.K., Milosavljevic M., Kasiuk J.V., Enhancement of negative capacitance effect in (FeCoZr)<sub>x</sub>(CaF<sub>2</sub>)<sub>(100-x)</sub> nanocomposite films deposited by ion beam sputtering in argon and oxygen atmosphere, *J. Alloys Compd.* 615 (2014), No 1, S361-S365.
- [13] Koltunowicz T.N., Żukowski P., Bondariev V., Fedotova J.A., Fedotov A.K., The effect of annealing on the impedance of (FeCoZr)<sub>x</sub>(CaF<sub>2</sub>)<sub>(100-x)</sub> nanocomposite films produced by the ion-beam sputtering in vacuum, *Vacuum*, (2015) DOI: 10.1016/j.vacuum.2015.01.030
- [14] Khomenko A.V., Lyashenko I.A., Borisjuk V.N. Self-similar phase dynamics of boundary friction. *Ukr. J. Phys.*, 54 (2009), No 11, 1139-1148.
- [15] Pogrebnjak A.D., Kobzev A.P., Gritsenko B.P., Sokolov S., Bazyl E., Sviridenko N.V., Valyaev A.N., Ivanov Y.F. Effect of Fe and Zr ion implantation and high-current electron irradiation treatment on chemical and mechanical properties of Ti-V-Al alloy. *J. Appl. Phys.*, 87 (2000), No 5, 2142-2148.
- [16] Pogrebnjak A.D., Beresnev V.M., Demianenko A.A., Baidak V.S., Komarov F.F., Kaverin M.V., Makhmudov N.A., Kolesnikov D.A. Adhesive strength, superhardness, and the phase and elemental compositions of nanostructured coatings based on Ti-Hf-Si-N. *Phys. Solid State*, 54 (2012), No 9, 1882-1890.
- [17] Svito I.A., Fedotova J.A., Milosavljević M., Zhukowski P., Koltunowicz T.N., Saad A., Kierczynski K., Fedotov A.K., Influence of sputtering atmosphere on hopping conductance in granular nanocomposite (FeCoZr)<sub>x</sub>(Al<sub>2</sub>O<sub>3</sub>)<sub>1-x</sub> films, *J. Alloys Compd.*, 615 (2014), No 1, S344-S347.

**Authors:** Prof. A.D. Pogrebnjak, Sumy State University, 40007, R.-Korsakova 2, Sumy, Ukraine, E-mail alexp@i.ua; Dr. O.V. Bondar, Sumy State University, 40007, R.-Korsakova 2, Sumy, Ukraine; Prof. N.K. Erdybaeva, East-Kazakhstan Technical University, 070004, Protozanov Str. 69, Ust-Kamenogorsk, Kazakhstan; Prof. S.V. Plotnikov, East-Kazakhstan Technical University, 070004, Protozanov Str. 69, Ust-Kamenogorsk, Kazakhstan; P.V. Turbin National Technical University "KhPI", 61002, Frunze Str. 21, Kharkiv, Ukraine; S.S. Grankin, Karazin Kharkiv National University, 61022, Svobody Sq. 4., Kharkiv, Ukraine; Dr. V.A. Stolbovoy, National Scientific Center "KhFTI", 61108, Academichna Str. 2, Kharkiv, Ukraine; Prof. O.V. Sobol, National Technical University "KhPI", 61002, Frunze Str. 21, Kharkiv, Ukraine; Prof. D.A. Kolesnikov, Belgorod State National Research University, Belgorod, Russian Federation; Dr. C. Kozak, Lublin University of Technology, 38d Nadbystrzycka Str., 20-618 Lublin, Poland.